

Luu, Duc Thi; Lux, Thomas

**Working Paper**

## Multilayer overlaps and correlations in the bank-firm credit network of Spain

Economics Working Paper, No. 2018-04

**Provided in Cooperation with:**

Christian-Albrechts-University of Kiel, Department of Economics

*Suggested Citation:* Luu, Duc Thi; Lux, Thomas (2018) : Multilayer overlaps and correlations in the bank-firm credit network of Spain, Economics Working Paper, No. 2018-04, Kiel University, Department of Economics, Kiel

This Version is available at:

<https://hdl.handle.net/10419/174871>

**Standard-Nutzungsbedingungen:**

Die Dokumente auf EconStor dürfen zu eigenen wissenschaftlichen Zwecken und zum Privatgebrauch gespeichert und kopiert werden.

Sie dürfen die Dokumente nicht für öffentliche oder kommerzielle Zwecke vervielfältigen, öffentlich ausstellen, öffentlich zugänglich machen, vertreiben oder anderweitig nutzen.

Sofern die Verfasser die Dokumente unter Open-Content-Lizenzen (insbesondere CC-Lizenzen) zur Verfügung gestellt haben sollten, gelten abweichend von diesen Nutzungsbedingungen die in der dort genannten Lizenz gewährten Nutzungsrechte.

**Terms of use:**

*Documents in EconStor may be saved and copied for your personal and scholarly purposes.*

*You are not to copy documents for public or commercial purposes, to exhibit the documents publicly, to make them publicly available on the internet, or to distribute or otherwise use the documents in public.*

*If the documents have been made available under an Open Content Licence (especially Creative Commons Licences), you may exercise further usage rights as specified in the indicated licence.*

# Multilayer Overlaps and Correlations in the Bank-Firm Credit Network of Spain

by Duc Thi Luu and Thomas Lux



# Multilayer Overlaps and Correlations in the Bank-Firm Credit Network of Spain\*

Duc Thi Luu<sup>1</sup> and Thomas Lux<sup>1</sup>

<sup>1</sup>*University of Kiel; Department of Economics; 24118 Kiel, Germany*

(Dated: Ver. January 15, 2018)

---

\* The first version of this paper has been completed while Thomas Lux held the Banco de España Chair in Computational Economics at the University of Jaume I, Castellón, Spain.  
Corresponding author: Thomas Lux, lux@economics.uni-kiel.de.

# Abstract

We investigate the structural dependencies in the bank-firm credit market of Spain under a multilayer network perspective. In particular, the original bipartite network is decomposed into different layers representing different industrial sectors. We then study the correlations between layers based on normalized measures of overlaps of links and weights of banks between layers. To assess the statistical significance of such correlations, we compare the observed values with the expected ones obtained from random graph models specifying only global constraints, i.e. the total degree or the total strength in single layers, and from configuration models capturing the intrinsic heterogeneity in the local constraints like the observed degree sequence and/or strength sequence in single layers. We find that, first, the raw dependencies between layers of the observed network are highly heterogeneous. Second, when evaluated against the null models, on the one hand, the rescaled correlations after filtering out the effects of the global constraints typically display no significant difference to the observed correlations. In addition, in the binary version, almost all correlations are still present after subtracting the effects of the observed degree sequences in all layers. On the other hand, the observed correlations are partially explained by the local constraints maintained in the weighted configuration models. All in all, comparing the observed network with all referenced null models, we find that the multilayer credit network under scrutiny has a significant, non-random structure of correlations that cannot be explained by more primitive network properties alone. In the binary case, such a non-random structure is, for instance, typically observed in the pairs of layers that have high levels of overlaps and correlations. In contrast, in the weighted case, patterns are found in different pairs of layers that have various levels of overlaps and correlations.

*JEL classification numbers: G11, G21*

*Keywords: Bank-Firm Credit Network; Multilayer Network; Multiplexity; Portfolio Overlaps; Correlations*

## I. INTRODUCTION

The recent financial crisis shows the danger of financial and economic links in propagating distress and creating systemic risk. Much of the analysis of risk contagion in the economic and financial system has so far focused on directed exposures in single mode networks (e.g. in the interbank lending network, in production networks). Less attention has, however, been devoted to the propagation of distress between the financial and the real sector of the economy.

In the last few years, there has been a growing interest in studying different channels of financial contagion by adding additional layers of connectivity within the network structure of the banking system. In a multilayer architecture, a failure of nodes in one layer may lead to other failures of connected nodes in other layers, and then the accumulated repercussion between all layers may eventually lead to a cascade of failures.

For example, in a model for systemic risk propagation in a bipartite network of banks' portfolio overlaps, the study of Huang et al. (2013) suggests that fluctuations in bank asset values may affect the financial robustness of a group of banks, and in turn it may force these banks to sell their assets. If this selling causes the market price of the assets to decrease, the balance sheets of all other banks who hold these assets will be affected due to mark-to-market evaluation. If this loss is large enough, further selling pressure may cause further devaluation of assets in the market. The failures may continue to spread to other banks and other assets and finally lead to a large decline of the banks' balance sheets as well as the capitalization in the assets market. In a similar study, Caccioli et al. (2014) develop a bank-asset bipartite network approach to amplification of financial contagion due to the combination of common asset holdings and leverage. Their findings suggest a "robust yet fragile" nature of the financial system. A higher degree of diversification in asset holdings of banks can create dangerous systemic effects, and too high leverage ratios can cause the unstable region of the financial network to grow.

Considering relationships between the banking system to non-financial firms, in a recent study, Lux (2016) suggests that to add bank-firm credit relations as a second important layer to a standard model of the interbank credit market. Although the bipartite structure in the bank-firm credit network is much sparser than in the interbank network, this does not imply that lending to non-financial firms should be of less concern from the viewpoint of

contagious spread of stress. Through computational experiments, his study suggests that in a certain number of cases, for instance due to a high local interlock between banks, a default of single business firms in the real sector may trigger a large scale collapse of the network.

There exist a small number of empirical studies on the bank-firm credit markets focusing on the topological properties of the aggregate bipartite structure or one-mode projection networks (e.g. De Masi et al., 2011; De Masi and Gallegati, 2012). However, such an aggregate perspective neglects the differences between various sectors of the real sphere of the economy and effectively treats credit to different sectors as perfect substitutes in banks' balance sheets. For instance, the issues of sectoral diversifications, sectoral overlaps, and sectoral correlations in banks' lending can not be addressed in such a setting. In fact, if we look at the portfolios of banks we can see that banks' lending distribution is diversified and that the lending strategies may also be heterogeneous. Some banks may prefer to diversify their portfolios, while others concentrate on a certain number of sectors and firms since they might have acquired expertise in lending, for example, due to lower costs of monitoring. To gain a deeper understanding of such differences, it is necessary to consider the multilayer structure of bank-firm credit relationships.

In the past few years, in network science, major advances in the understanding of the statistical properties and mechanics of multilayer networks have been made. Among others, the issue of overlaps and dependencies between layers has received significant attention since it is important to understand the interactions between layers (e.g. Bianconi, 2014; Boccaletti et al., 2014; Menichetti, Remondini, and Bianconi, 2014; Menichetti et al., 2014; Kivela et al., 2014). It is commonly observed that the robustness of a multiplex network is significantly affected by the interactions between its layers (e.g. Bianconi, 2014; Chen et al., 2015; Menichetti et al., 2016).

Among a limited number of empirical studies on economic and financial multiplex networks, probably the International Trade Network (ITN) has been studied most intensively due to advantages in data availability [1]. For instance, Barigozzi et al. (2010) decompose the ITN into almost 100 layers based on commodity codes. Their findings show that the distributions of link weights in single layers are highly heterogeneous, and the network properties at commodity levels are very different from those of the aggregated one. In addition, the analysis of cross-layer correlations suggests that the ITN is not simply an aggregate network of many independent layers.

In order to assess the statistical significance of network properties, one needs to compare the observed properties with those of an appropriate null model. To construct such null models for multilayer networks, Mastrandrea et al. (2014b) adopt the benchmark of the so-called configuration models (e.g. Squartini et al., 2011a; Squartini et al., 2011b; Mastrandrea et al., 2014a; Squartini et al., 2015) to investigate the role of local constraints like the degree distribution and the strength distribution in replicating some structural correlations of the World Trade multiplex. Decomposing the aggregate trade network into nearly 100 commodity specific layers, their findings indicate that the main features of the structural correlations like average nearest neighbor degrees as well as clustering coefficients are well replicated at both the layer and aggregate levels by the local constraints. Two recent studies of Gemmetto and Garlaschilli (2015), Gemmetto et al. (2015) have applied multiplexity measures to the International Trade Network as well as the European Airport Network, and then compare these networks with random graph models and configuration models including the so called binary configuration model (Squartini et al., 2011a) and the so called weighted configuration model (Squartini et al., 2011b). Gemmetto and Garlaschilli (2015) and Gemmetto et al. (2015) show that the local constraints in single layers such as the degree sequence and the strength sequence play an important role in explaining the dependencies between layers, highlighting the important role played by the hubs across layers. Their findings also suggest that the use of homogeneous benchmarks (i.e. the family of random graph models), which treat all agents as homogeneous in each layer, can lead to misleading results.

Following recent advances in the study of multiplex networks (e.g. Bianconi, 2013; Gemmetto and Garlaschilli, 2015; Gemmetto et al., 2015), in our paper we will analyze the bank-firm credit network of Spain with a focus on the overlaps and correlations between layers representing industrial sectors of firms [2]. In particular, we investigate whether the observed correlations between layers differ significantly from the expected values obtained from random graph models specifying only global constraints and from configuration models preserving the intrinsic heterogeneity in the degree sequence and/or strength sequence of the observed network. Our aims are twofold: (i) to investigate the role of different constraints in explaining the dependencies between layers in the observed multiplex network; and (ii) to identify the presence of patterns in such dependencies. Regarding the null models, we add an important novelty to the theoretical framework for measuring multiplexity in mul-

tilayer networks, namely the rescaled multiplexity evaluated under the so-called enhanced configuration model (ECM) where both the observed degree as well as strength sequences are enforced in each layer.

The remainder of this paper is structured as follows. In Sec. II we briefly describe the methods used for measuring the overlaps and multiplexity in a multilayer network. Sec. III reports our main findings for the bank-firm credit market of Spain. Discussions and concluding remarks are in Sec. IV. At the end of this paper, the Appendix provides an outline of the assessment of significance of multiplex features under the ECM.

## II. OVERLAPS AND MULTIPLEXITY IN MULTILAYER NETWORKS

### A. General definitions, measures for overlaps, and null models

In this part, first, we briefly define some basic notations and definitions of a multiplex network. After that we will explain the method used to quantify the overlaps between layers. Basically, we follow the approach proposed in Bianconi (2013) and in Menichetti et al. (2014), respectively, for binary and weighted multiplex networks [3]. Next, we introduce different null models employed in this study including the family of random graph models and the family of configuration models.

#### 1. General definitions

Generally, suppose we have  $N$  nodes and  $NS$  layers such that nodes may be connected with others in any layer. A generic multiplex can be defined by  $\vec{G} = (G^1, G^2, \dots, G^\alpha, \dots, G^{NS})$ , where the network of each layer  $\alpha$ , namely  $G^\alpha$ , is characterized by a binary adjacency matrix  $A_\alpha = \{a_{ij}^\alpha\}$  and/or a weighted matrix  $W_\alpha = \{w_{ij}^\alpha\}$ , where  $i, j$  are indexed from 1 to  $N$  representing the  $N$  nodes in the network. It should be noted that, in an undirected network, the adjacency and weighted matrices are symmetric.

Similar to elementary one-mode networks, we define the degree and strength of node  $i$  in each layer  $\alpha = 1, 2, \dots, NS$  as the (unweighted and weighted) sums of their links:

$$k_i^\alpha = \sum_{j \neq i} a_{ij}^\alpha, \quad (1)$$

$$s_i^\alpha = \sum_{j \neq i} w_{ij}^\alpha. \quad (2)$$



The total number of links  $L^\alpha$  and total weight  $W^\alpha$  in layer  $\alpha$  in an undirected network are given by

$$L^\alpha = \sum_i \sum_{i < j} a_{ij}^\alpha, \quad (3)$$

$$W^\alpha = \sum_i \sum_{i < j} w_{ij}^\alpha. \quad (4)$$

Now, we will relate the above definitions to our particular data, i.e. the bank-firm credit network. Assume that we have a binary, undirected, bipartite credit network without sectoral differentiation of  $N$  banks lending to  $F$  firms in  $NS$  sectors. We define the adjacency matrix of that network as

$$A^{B-F} = \{a_{ij}^{b-f}\}_{N \times F} \quad (5)$$

where  $a_{ij}^{b-f} = 1$  if bank  $i$  lends to firm  $j$ , and zero otherwise. The degrees of bank  $i$  and firm  $j$  in the bank-firm credit network without sectoral differentiation are respectively given by

$$k_{bf}(i) = \sum_{k=1}^F a_{ik}^{b-f} \quad (6)$$

and

$$k_{fb}(j) = \sum_{k=1}^B a_{kj}^{b-f}. \quad (7)$$

Considering bank-sector relations, we define the adjacency matrix of the bipartite bank-sector credit network consisting of  $N$  banks and  $NS$  sectors as

$$M^{B-S} = \{m_{ij}^{b-s}\}_{N \times NS} \quad (8)$$

where  $m_{ij}^{b-s} = 1$  if bank  $i$  lends to at least one firm in sector  $j$ , and zero otherwise.

Denote

$$k_{bs}(i) = \sum_{j=1}^{NS} m_{ij}^{b-s}, \quad (9)$$

$$k_{sb}(j) = \sum_{i=1}^N m_{ij}^{b-s}, \quad (10)$$

respectively the degrees of bank  $i$  and sector  $j$  in the bank-sector credit network.

The degrees  $k_{bf}$  and  $k_{bs}$  indicate, respectively, the diversification in the loan portfolio of banks at firm and sector levels, while the degrees  $k_{sb}$  and  $k_{fb}$  show the diversification in borrowing of firms and sectors respectively.

In addition, we can decompose the original bank-firm credit network  $A^{B-F}$  into bank-firm lending relations in a particular sector.  $M^{B-F,\alpha} = \{m_{ij}^{b-f,\alpha}\}_{N \times F_\alpha}$  denotes the adjacency matrix showing the credit relations between banks and firms in each sector  $\alpha$ , where  $m_{ij}^{b-f,\alpha} = 1$  if bank  $i$  lends to firm  $j$  in sector  $\alpha$  and zero otherwise; and  $F_\alpha$  is the number of firms in sector  $\alpha$ .

From the adjacency matrix of each sector  $\alpha$ , we obtain a network structure of joint exposures of banks by projecting the bipartite bank-firm network  $M^{B-F,\alpha}$  onto an undirected bank-bank network with an adjacency matrix  $A_\alpha = \{a_{ij}^\alpha\}_{N \times N}$  and a weighted matrix  $W_\alpha = \{w_{ij}^\alpha\}_{N \times N}$  as mentioned at the beginning of this subsection.

Note that, from the economic point of view,  $a_{ij}^\alpha = 1$  if there is a firm in sector  $\alpha$  that two banks  $i$  and  $j$  co-finance. In addition,  $w_{ij}^\alpha$  is nothing else but the total number of common borrowers in sector  $\alpha$  of two banks  $i$  and  $j$ . In addition,  $k_i^\alpha$  (Eq. (1)) and  $S_i^\alpha$  (Eq. (2)), respectively, indicate the degree and the strength of bank  $i$  in the layer  $\alpha$ . Consequently, the aggregate bank-firm credit network is now reduced to a multiplex network of  $N$  banks in  $NS$  layers, and each of  $NS$  layers shows the overlaps between the  $N$  banks in their lending to the industrial sector of firms associated to that layer.

## 2. Measures for overlaps

For two different layers  $\alpha$  and  $\beta$ , the overall binary overlap is given by

$$O_{bin}^{\alpha,\beta} = \sum_i \sum_{i < j} a_{ij}^\alpha a_{ij}^\beta. \quad (11)$$

The local binary overlap for node  $i$  in two layers  $\alpha, \beta$  is defined as

$$o_{i,bin}^{\alpha,\beta} = \sum_{j \neq i} a_{ij}^\alpha a_{ij}^\beta. \quad (12)$$

Another way to define the overlaps between layers is based on the minimum values of the elements in two adjacency matrices. These measures are proposed by Gemmetto and Garlaschelli (2015). More specifically, the overall binary overlap between two layers  $\alpha$  and  $\beta$  is given by

$$O_{bin}^{\alpha,\beta} = \sum_i \sum_{i < j} \min(a_{ij}^\alpha, a_{ij}^\beta). \quad (13)$$

It is easy to show that  $\min(a_{ij}^\alpha, a_{ij}^\beta) = a_{ij}^\alpha a_{ij}^\beta$ , consequently Eq. (11) and Eq. (13) are equivalent. Similarly, ones can also define the local binary overlap for node  $i$  as

$$o_{i,bin}^{\alpha,\beta} = \sum_{j \neq i} \min(a_{ij}^\alpha, a_{ij}^\beta), \quad (14)$$

which is again identical to Eq. (12).

For weighted networks, both definitions do lead to different measurements, and it is mainly the second version that is intuitively appealing. The overall weighted overlap between two layers  $\alpha$  and  $\beta$  is then defined as

$$O_w^{\alpha,\beta} = \sum_i \sum_{i < j} \min(w_{ij}^\alpha, w_{ij}^\beta). \quad (15)$$

The local weighted overlap for node  $i$  in two layers  $\alpha, \beta$  is defined as

$$o_{i,w}^{\alpha,\beta} = \sum_{j \neq i} \min(w_{ij}^\alpha, w_{ij}^\beta). \quad (16)$$

The overlap coefficients indicate the similarities between layers. In the binary case, while  $O_{bin}^{\alpha,\beta}$  is the total number of pairs of nodes linked at the same time by an edge in layer  $\alpha$  and an edge in layer  $\beta$ , the local measure  $o_{i,bin}^{\alpha,\beta}$  is the total number of other nodes connected to node  $i$  at the same time by an edge in  $\alpha$  and an edge in layer  $\beta$ . The overall weighted overlap  $O_w^{\alpha,\beta}$  and the local weighted overlap  $o_{i,w}^{\alpha,\beta}$  are interpreted in a similar way but they take into account the weights of the links in both layers  $\alpha$  and  $\beta$ . Based on these definitions, in the next subsection we will define the raw binary multiplexity and the raw weighted multiplexity showing the correlations between layers in a multilayer network.

### 3. Null models

The seminal work of Bianconi (2013) provides a framework for the formal characterization of correlated multiplex ensembles satisfying certain constraints. Accordingly, in a multiplex ensemble, where the probability for each possible outcome is specified by  $P(\vec{G})$ , the (overall) entropy of the multiplex is defined as

$$S = - \sum_{\vec{G}} P(\vec{G}) \ln P(\vec{G}). \quad (17)$$

In the case of an uncorrelated multiplex, i.e., if the correlation between any two separate layers is equal to zero, we can decompose the overall entropy in Eq. (17) into the sum of the single layers' entropy

$$S = \sum_{\alpha=1}^{NS} S^\alpha = - \sum_{\alpha=1}^{NS} P_\alpha(G^\alpha) \ln P_\alpha(G^\alpha) \quad (18)$$

since we have

$$P(\vec{G}) = \prod_{\alpha=1}^{NS} P_\alpha(G^\alpha) \quad (19)$$

where  $P_\alpha(G^\alpha)$  is the probability of  $G^\alpha$  in the layer  $\alpha$ . In contrast, if layers are correlated, we can not factorize the overall entropy as in Eq. (18).

We follow the ideas of Gemmetto and Garlaschelli (2015) and Gemmetto et al. (2015) to consider the role of constraints in single layers on correlations between layers of a multiplex network. For instance, for each layer  $\alpha$  of a multiplex network that we have defined above, we may want to preserve the total degree  $L^\alpha$ , or the degree sequence  $\{k_i^\alpha\}_{i=1}^{i=N}$ , or the total weight  $W^\alpha$ , or the strength sequence  $\{S_i^\alpha\}_{i=1}^{i=N}$ , or both  $\{k_i^\alpha\}_{i=1}^{i=N}$  as well as  $\{S_i^\alpha\}_{i=1}^{i=N}$ .

Recent studies (e.g. Squartini et al., 2011a; Squartini et al., 2011b; Mastrandrea et al., 2014a; Squartini et al., 2015) provide a general method for unbiased randomizing ensembles for different versions of networks with various constraints. Based on maximum entropy and maximum likelihood methods, hidden variables are analytically extracted from the initially given constraints. In the following, we briefly introduce the family of random graph models and the family of configuration models. The main difference between both families is that in the former, we specify only global constraints and therefore treat all nodes in the network homogeneously, while in the latter the intrinsic heterogeneity in the degree and/or strength distributions is maintained.

#### *Random Graph models*

In the undirected Binary Random Graph model (BRG), with the total degree  $L^\alpha$  of  $N$  nodes in each layer  $\alpha$ , the probability of a link between any two different nodes in that layer is given by

$$p^\alpha = \frac{2L^\alpha}{N(N-1)} = \langle a_{ij}^\alpha \rangle_{BRG}, \quad (20)$$

where  $\langle a_{ij}^\alpha \rangle_{BRG}$  is the notation for the expectation of  $a_{ij}^\alpha$  under the BRG model [4].

In the undirected Weighted Random Graph model (WRG), the total strength  $W^\alpha$  of  $N$  nodes in each layer  $\alpha$ , the probability of a link of weight  $w_{ij}^\alpha$  between any two different nodes (i, j) in the layer  $\alpha$  is equal to

$$q(w_{ij}^\alpha) = \begin{cases} 1 - p_w^\alpha, & \text{if } w_{ij}^\alpha = 0, \\ (p_w^\alpha)^{w_{ij}^\alpha} (1 - p_w^\alpha), & \text{if } w_{ij}^\alpha > 0, \end{cases} \quad (21)$$

where the parameter  $p_w^\alpha$  is given by

$$p_w^\alpha = \frac{2W^\alpha}{N(N-1) + 2W^\alpha}. \quad (22)$$

The expected link weight between node  $i$  and node  $j$  is

$$\langle w_{ij}^\alpha \rangle_{WRG} = \frac{2W^\alpha}{N(N-1)}. \quad (23)$$

The probability of a link between node  $i$  and node  $j$  is

$$\langle a_{ij}^\alpha \rangle_{WRG} = p_w^\alpha = \frac{2W^\alpha}{N(N-1) + 2W^\alpha}. \quad (24)$$

### *Configuration models*

We now move on to configuration models that preserve the degree and/or strength sequence of a given network.

In the undirected Binary Configuration model (BCM), in each layer  $\alpha$ , the degree sequence  $\{k_i^\alpha\}_{i=1}^N$  is given. Mathematically, we then need to solve a system of  $N$  equations in each layer  $\alpha$  to obtain  $N$  non-negative hidden variables  $\{x_i^\alpha\}_{i=1}^N$  that determine the link formation probability

$$\sum_{j \neq i} \frac{x_i^\alpha x_j^\alpha}{1 + x_i^\alpha x_j^\alpha} = k_i^\alpha, \forall i = 1, 2, \dots, N. \quad (25)$$

The probability of a link between node  $i$  and node  $j$  in layer  $\alpha$  is given by

$$\langle a_{ij}^\alpha \rangle_{BCM} = p_{ij}^\alpha = \frac{x_i^\alpha x_j^\alpha}{1 + x_i^\alpha x_j^\alpha}. \quad (26)$$

In the undirected Weighted Configuration model (WCM), in each layer  $\alpha$ , the strength sequence  $\{s_i^\alpha\}_{i=1}^N$  is given. Hidden variables  $\{x_i^\alpha\}_{i=1}^N \in [0, 1)$  associated with  $N$  nodes are again obtained by solving

$$\sum_{j \neq i} \frac{x_i^\alpha x_j^\alpha}{1 - x_i^\alpha x_j^\alpha} = s_i^\alpha, \forall i = 1, 2, \dots, N. \quad (27)$$

The probability of a link of weight  $w_{ij}^\alpha$  between node  $i$  and node  $j$  in the WCM is

$$q(w_{ij}^\alpha) = \begin{cases} 1 - p_{ij}^\alpha, & \text{if } w_{ij}^\alpha = 0, \\ (p_{ij}^\alpha)^{w_{ij}^\alpha} (1 - p_{ij}^\alpha), & \text{if } w_{ij}^\alpha > 0, \end{cases} \quad (28)$$

where

$$p_{ij}^\alpha = x_i^\alpha x_j^\alpha. \quad (29)$$

The expected link weight between node  $i$  and node  $j$  is given by

$$\langle w_{ij}^\alpha \rangle_{WCM} = \frac{x_i^\alpha x_j^\alpha}{1 - x_i^\alpha x_j^\alpha}. \quad (30)$$

The probability of a link between node  $i$  and node  $j$  in layer  $\alpha$  is specified as

$$\langle a_{ij}^\alpha \rangle_{WCM} = p_{ij}^\alpha = x_i^\alpha x_j^\alpha. \quad (31)$$

In the undirected Enhanced Configuration model (ECM), in each layer  $\alpha$ , the degree sequence  $\{k_i^\alpha\}_{i=1}^N$  as well as the strength sequence  $\{s_i^\alpha\}_{i=1}^N$  are given. The non-negative variables  $\{x_i^\alpha\}_{i=1}^N$  and  $\{y_i^\alpha\}_{i=1}^N$  ( $\{y_i^\alpha\}_{i=1}^N \in [0, 1]$ ) are the solution to the system of  $2N$  equations

$$\begin{aligned} \sum_{j \neq i} \frac{x_i^\alpha x_j^\alpha y_i^\alpha y_j^\alpha}{1 - y_i^\alpha y_j^\alpha + x_i^\alpha x_j^\alpha y_i^\alpha y_j^\alpha} &= k_i^\alpha, \forall i = 1, 2, \dots, N, \\ \sum_{j \neq i} \frac{x_i^\alpha x_j^\alpha y_i^\alpha y_j^\alpha}{(1 - y_i^\alpha y_j^\alpha)(1 - y_i^\alpha y_j^\alpha + x_i^\alpha x_j^\alpha y_i^\alpha y_j^\alpha)} &= s_i^\alpha, \forall i = 1, 2, \dots, N. \end{aligned} \quad (32)$$

The probability a link of weight  $w_{ij}^\alpha$  is now given by

$$q(w_{ij}^\alpha) = \begin{cases} 1 - p_{ij}^\alpha, & \text{if } w_{ij}^\alpha = 0, \\ p_{ij}^\alpha r_{ij,\alpha}^{w_{ij}^\alpha - 1} (1 - r_{ij,\alpha}), & \text{if } w_{ij}^\alpha > 0, \end{cases} \quad (33)$$

where

$$p_{ij}^\alpha = \frac{x_i^\alpha x_j^\alpha y_i^\alpha y_j^\alpha}{1 - y_i^\alpha y_j^\alpha + x_i^\alpha x_j^\alpha y_i^\alpha y_j^\alpha}, \quad (34)$$

and

$$r_{ij,\alpha} = y_i^\alpha y_j^\alpha. \quad (35)$$

The expected link weight between node  $i$  and node  $j$  is given by

$$\langle w_{ij}^\alpha \rangle_{ECM} = \frac{x_i^\alpha x_j^\alpha y_i^\alpha y_j^\alpha}{(1 - y_i^\alpha y_j^\alpha)(1 - y_i^\alpha y_j^\alpha + x_i^\alpha x_j^\alpha y_i^\alpha y_j^\alpha)}, \quad (36)$$

and the probability of a link between node  $i$  and node  $j$  is

$$\langle a_{ij}^\alpha \rangle_{ECM} = p_{ij}^\alpha = \frac{x_i^\alpha x_j^\alpha y_i^\alpha y_j^\alpha}{1 - y_i^\alpha y_j^\alpha + x_i^\alpha x_j^\alpha y_i^\alpha y_j^\alpha}. \quad (37)$$

One important result of the configuration models is that, mathematically, the expected values of the properties of networks over the ensemble can be calculated via hidden variables (see, for instance, Squartini and Garlaschelli, 2011; Squartini et al., 2015). In addition, in a multilayer network, the expected values of the overlaps and correlations between layers still depend on the properties of the expected adjacency matrices (in the binary case) as well as the expected weighted matrices (in the weighted case), and they can analytically be computed based on hidden variables extracted in the single layers (Gemmetto and Garlaschelli, 2015; Gemmetto et al., 2015). In the following subsection, we will show how to measure the expected and rescaled multiplexities under the various null models.

## B. Multiplexity

We will in the following, first define the multiplexities of an observed multilayer network, and then introduce the expectation for these measures under the various null models. In addition, to assess the statistical significance of the observed multiplexities, we employ the analysis of z-scores indicating the difference between the observed and the expected multiplexities in units of the standard deviation of the pertinent measure under any null model.

For a more detailed description and proof for the expected multiplexities and z-scores under the BRG model, the BCM, the WRG model, and the WCM, we refer the readers to the study of Gemmetto and Garleaschelli (2015). We add the analytical details for the ECM in the Appendix.

### 1. Undirected binary multiplexity

#### *Raw binary multiplexity*

For binary network, the raw (observed) multiplexity between two layers  $\alpha$  and  $\beta$  is defined as

$$m_{bin}^{\alpha,\beta} = \frac{2 \sum_i \sum_{i < j} \min(a_{ij}^\alpha, a_{ij}^\beta)}{L^\alpha + L^\beta}. \quad (38)$$

The multiplexity indicator between any two layers  $\alpha$  and  $\beta$  ranges in  $[0,1]$ , and it is maximally equal to 1 if  $\alpha$  and  $\beta$  are identical, and minimally equal to 0 when there is no overlap between the two layers. Clearly, the raw binary multiplexity is actually based on the overall overlap between two layers as achieved in Eq. (13). The only difference here is the term  $\frac{L^\alpha + L^\beta}{2}$ , which is used to normalize  $O_{bin}^{\alpha,\beta}$ .

We rescale this measured multiplexity by

$$\mu_{bin}^{\alpha,\beta} = \frac{m_{bin}^{\alpha,\beta} - \langle m_{bin}^{\alpha,\beta} \rangle}{1 - \langle m_{bin}^{\alpha,\beta} \rangle}, \quad (39)$$

where  $\langle m_{bin}^{\alpha,\beta} \rangle$  is the expected value of the binary multiplexity under the chosen null model. This rescaled multiplexity measures the relative difference between the observed multiplexity and the expected one with respect to the referenced null model. It is easy to show that  $\mu_{bin}^{\alpha,\beta} < 1$ .

Mathematically, the general formulation of  $\langle m_{bin}^{\alpha,\beta} \rangle$  is given by

$$\langle m_{bin}^{\alpha,\beta} \rangle = \frac{2 \sum_i \sum_{i < j} \langle \min(a_{ij}^\alpha, a_{ij}^\beta) \rangle}{L^\alpha + L^\beta}. \quad (40)$$

In the binary case, it can be shown that

$$\langle \min(a_{ij}^\alpha, a_{ij}^\beta) \rangle = p_{ij}^\alpha p_{ij}^\beta, \quad (41)$$

where  $p_{ij}^\alpha$  is the probability of a link between nodes  $i$  and  $j$  in layer  $\alpha$ . It should be noted that under different null models (i.e. BRG, BCM),  $p_{ij}^\alpha$  will have different forms.

#### *Binary z score*

While the rescaled quantities can explain the similarity between layers, we still need another measure that shows how much the raw value  $m_{bin}^{\alpha,\beta}$  deviates from the expected value  $\langle m_{bin}^{\alpha,\beta} \rangle$ . This leads to the definition of the z score of  $m_{bin}^{\alpha,\beta}$  (binary z score in short) under the chosen null model, which is given by

$$z[m_{bin}^{\alpha,\beta}] = \frac{m_{bin}^{\alpha,\beta} - \langle m_{bin}^{\alpha,\beta} \rangle}{\sigma[m_{bin}^{\alpha,\beta}]}, \quad (42)$$

where  $\sigma[m_{bin}^{\alpha,\beta}]$  is the standard deviation of  $m_{bin}^{\alpha,\beta}$  [5].

Note that

$$\sigma[m_{bin}^{\alpha,\beta}] = \frac{2\sigma[\sum_i \sum_{i<j} \min\{a_{ij}^\alpha, a_{ij}^\beta\}]}{L^\alpha + L^\beta}, \quad (43)$$

and

$$\sigma^2[\min\{a_{ij}^\alpha, a_{ij}^\beta\}] = \langle \min\{a_{ij}^\alpha, a_{ij}^\beta\}^2 \rangle - \langle \min\{a_{ij}^\alpha, a_{ij}^\beta\} \rangle^2. \quad (44)$$

In the following, we will consider the rescaled quantity and the z-score in two particular cases, i.e. under the BRG model and under the BCM.

–Under BRG model

Under the BRG model, it can be shown that

$$\langle \min\{a_{ij}^\alpha, a_{ij}^\beta\} \rangle_{BRG} = p^\alpha p^\beta, \quad (45)$$

where for each layer  $\alpha$ ,  $p^\alpha = \frac{2L^\alpha}{N(N-1)}$  as in Eq. (20).

The expectation of  $m_{bin}^{\alpha,\beta}$  under the BRG model is then

$$\langle m_{bin}^{\alpha,\beta} \rangle_{BRG} = \frac{2 \sum_i \sum_{i<j} p^\alpha p^\beta}{L^\alpha + L^\beta}. \quad (46)$$

Defining  $\mu_{BRG}^{\alpha,\beta}$  as the rescaled multiplexity under the BRG model, we have

$$\mu_{BRG}^{\alpha,\beta} = \frac{2 \sum_i \sum_{i<j} \min(a_{ij}^\alpha, a_{ij}^\beta) - 2 \sum_i \sum_{i<j} p^\alpha p^\beta}{L^\alpha + L^\beta - 2 \sum_i \sum_{i<j} p^\alpha p^\beta}. \quad (47)$$



Note that, according to Gemmetto and Garleaschelli (2015), the rescaled multiplexity under the BRG model in fact can be reduced to the usual correlation coefficient between the elements of the adjacency matrix for any pair of layers  $\alpha$  and  $\beta$ .

In addition, under the BRG model we have

$$\sigma[\min\{a_{ij}^\alpha, a_{ij}^\beta\}]_{BRG} = \sqrt{p^\alpha p^\beta - (p^\alpha p^\beta)^2}. \quad (48)$$

Therefore, we obtain the z-score of  $m_{bin}^{\alpha,\beta}$  under the BRG model as

$$z_{BRG}^{\alpha,\beta} = \frac{\sum_i \sum_{i<j} \min\{a_{ij}^\alpha, a_{ij}^\beta\} - \sum_i \sum_{i<j} p^\alpha p^\beta}{\sqrt{\sum_i \sum_{i<j} [p^\alpha p^\beta - (p^\alpha p^\beta)^2]}}. \quad (49)$$

–Under the BCM

Under the BCM, it can be shown that

$$\langle \min\{a_{ij}^\alpha, a_{ij}^\beta\} \rangle_{BCM} = p_{ij}^\alpha p_{ij}^\beta, \quad (50)$$

where as mentioned in Eq. (26),  $p_{ij}^\alpha = \frac{x_i^\alpha x_j^\alpha}{1+x_i^\alpha x_j^\alpha}$  for each layer  $\alpha$ .

That leads to the following expression for the expectation of  $m_{bin}^{\alpha,\beta}$  under the BCM

$$\langle m_{bin}^{\alpha,\beta} \rangle_{BCM} = \frac{2 \sum_i \sum_{i<j} p_{ij}^\alpha p_{ij}^\beta}{L^\alpha + L^\beta}. \quad (51)$$

Therefore, we have

$$\mu_{BCM}^{\alpha,\beta} = \frac{2 \sum_i \sum_{i<j} \min(a_{ij}^\alpha, a_{ij}^\beta) - 2 \sum_i \sum_{i<j} p_{ij}^\alpha p_{ij}^\beta}{L^\alpha + L^\beta - 2 \sum_i \sum_{i<j} p_{ij}^\alpha p_{ij}^\beta}, \quad (52)$$

where  $\mu_{BCM}^{\alpha,\beta}$  as the rescaled multiplexity under the BCM model.

Additionally, the standard deviation of  $\min\{a_{ij}^\alpha, a_{ij}^\beta\}$  is given by

$$\sigma[\min\{a_{ij}^\alpha, a_{ij}^\beta\}]_{BCM} = \sqrt{p_{ij}^\alpha p_{ij}^\beta - (p_{ij}^\alpha p_{ij}^\beta)^2}. \quad (53)$$

From that, we obtain the z-score of  $m_{bin}^{\alpha,\beta}$  under the BCM model as

$$z_{BCM}^{\alpha,\beta} = \frac{\sum_i \sum_{i<j} \min\{a_{ij}^\alpha, a_{ij}^\beta\} - \sum_i \sum_{i<j} p_{ij}^\alpha p_{ij}^\beta}{\sqrt{\sum_i \sum_{i<j} [p_{ij}^\alpha p_{ij}^\beta - (p_{ij}^\alpha p_{ij}^\beta)^2]}}. \quad (54)$$

## 2. Undirected weighted multiplexity

*Raw weighted multiplexity*

For undirected weighted multiplexities, similar to the binary case, we start by defining the generic weighted multiplexity as

$$m_w^{\alpha,\beta} = \frac{2 \sum_i \sum_{i < j} \min(w_{ij}^\alpha, w_{ij}^\beta)}{W^\alpha + W^\beta}. \quad (55)$$

The interpretation for  $m_w^{\alpha,\beta}$  is similar to that for  $m_{bin}^{\alpha,\beta}$ , but here we take into account the role of link weights between nodes in every layer.

#### *Rescaled weighted multiplexity*

The rescaled quantity for  $m_w^{\alpha,\beta}$  is defined as

$$\mu_w^{\alpha,\beta} = \frac{m_w^{\alpha,\beta} - \langle m_w^{\alpha,\beta} \rangle}{1 - \langle m_w^{\alpha,\beta} \rangle}, \quad (56)$$

where  $\langle m_w^{\alpha,\beta} \rangle$  is the expected value under the referenced null model.

Mathematically,  $\langle m_w^{\alpha,\beta} \rangle$  can generally be expressed as

$$\langle m_w^{\alpha,\beta} \rangle = \frac{2 \sum_i \sum_{i < j} \langle \min(w_{ij}^\alpha, w_{ij}^\beta) \rangle}{W^\alpha + W^\beta}. \quad (57)$$

#### *Weighted z scores*

Similar to the binary case, weighted z scores can tell us how many standard deviations the raw weighted multiplexity differs from the expected value under the considered null model. The general form for the z-score of weighted multiplexity (weighted z-score in short) is defined as

$$z[m_w^{\alpha,\beta}] = \frac{m_w^{\alpha,\beta} - \langle m_w^{\alpha,\beta} \rangle}{\sigma[m_w^{\alpha,\beta}]}. \quad (58)$$

In addition, in general, we have that

$$\sigma[m_w^{\alpha,\beta}] = \frac{\sigma[\sum_i \sum_{i < j} \min\{w_{ij}^\alpha, w_{ij}^\beta\}]}{W^\alpha + W^\beta}, \quad (59)$$

and

$$\sigma^2[\min\{w_{ij}^\alpha, w_{ij}^\beta\}] = \langle \min\{w_{ij}^\alpha, w_{ij}^\beta\}^2 \rangle - \langle \min\{w_{ij}^\alpha, w_{ij}^\beta\} \rangle^2. \quad (60)$$

–Under the WRG model

Under the WRG model, it can be shown that

$$\langle \min(w_{ij}^\alpha, w_{ij}^\beta) \rangle_{WRG} = \frac{p_w^\alpha p_w^\beta}{1 - p_w^\alpha p_w^\beta}, \quad (61)$$

where  $p_w^\alpha = \frac{2W^\alpha}{N(N-1)+2W^\alpha}$  for each layer  $\alpha$  as in Eq. (24).

We then obtain

$$\langle m_w^{\alpha,\beta} \rangle_{WRG} = \frac{2 \sum_i \sum_{i < j} \frac{p_w^\alpha p_w^\beta}{(1 - p_w^\alpha p_w^\beta)}}{W^\alpha + W^\beta}. \quad (62)$$

The rescaled quantity for  $m_w^{\alpha,\beta}$  under the WRG models is then specified by

$$\mu_{WRG}^{\alpha,\beta} = \frac{2 \sum_i \sum_{i < j} \min \{w_{ij}^\alpha, w_{ij}^\beta\} - 2 \sum_i \sum_{i < j} \frac{p_w^\alpha p_w^\beta}{(1 - p_w^\alpha p_w^\beta)}}{W^\alpha + W^\beta - 2 \sum_i \sum_{i < j} \frac{p_w^\alpha p_w^\beta}{(1 - p_w^\alpha p_w^\beta)}}. \quad (63)$$

In addition, we have

$$\sigma[\min\{w_{ij}^\alpha, w_{ij}^\beta\}]_{WRG} = \sqrt{\frac{p_w^\alpha p_w^\beta}{(1 - p_w^\alpha p_w^\beta)^2}}. \quad (64)$$

Therefore, the z-score under the WRG model is expressed as

$$z_{WRG}^{\alpha,\beta} = \frac{\sum_i \sum_{i < j} \min \{w_{ij}^\alpha, w_{ij}^\beta\} - \sum_i \sum_{i < j} \frac{p_w^\alpha p_w^\beta}{(1 - p_w^\alpha p_w^\beta)}}{\sqrt{\sum_i \sum_{i < j} \left[ \frac{p_w^\alpha p_w^\beta}{(1 - p_w^\alpha p_w^\beta)^2} \right]}}. \quad (65)$$

–Under the WCM

Under the WCM, we have that

$$\langle \min(w_{ij}^\alpha, w_{ij}^\beta) \rangle_{WCM} = \frac{p_{ij}^\alpha p_{ij}^\beta}{1 - p_{ij}^\alpha p_{ij}^\beta}, \quad (66)$$

where  $p_{ij}^\alpha = x_i^\alpha x_j^\alpha$  as in Eq. (31).

The expected multiplexity under the WCM is then given by

$$\langle m_w^{\alpha,\beta} \rangle_{WCM} = \frac{2 \sum_i \sum_{i < j} \frac{p_{ij}^\alpha p_{ij}^\beta}{(1 - p_{ij}^\alpha p_{ij}^\beta)}}{W^\alpha + W^\beta}. \quad (67)$$

Therefore, the rescaled multiplexity in the WCM is specified as

$$\mu_{WCM}^{\alpha,\beta} = \frac{2 \sum_i \sum_{i < j} \min \{w_{ij}^\alpha, w_{ij}^\beta\} - 2 \sum_i \sum_{i < j} \frac{p_{ij}^\alpha p_{ij}^\beta}{(1 - p_{ij}^\alpha p_{ij}^\beta)}}{W^\alpha + W^\beta - 2 \sum_i \sum_{i < j} \frac{p_{ij}^\alpha p_{ij}^\beta}{(1 - p_{ij}^\alpha p_{ij}^\beta)}}. \quad (68)$$

Moreover, it can be shown that

$$\sigma[\min\{w_{ij}^\alpha, w_{ij}^\beta\}]_{WCM} = \sqrt{\frac{p_{ij}^\alpha p_{ij}^\beta}{(1 - p_{ij}^\alpha p_{ij}^\beta)^2}}. \quad (69)$$

We obtain the following expression for the z-score under the WCM

$$z_{WCM}^{\alpha,\beta} = \frac{\sum_i \sum_{i<j} \min\{w_{ij}^\alpha, w_{ij}^\beta\} - \sum_i \sum_{i<j} \frac{p_{ij}^\alpha p_{ij}^\beta}{(1-p_{ij}^\alpha p_{ij}^\beta)}}{\sqrt{\sum_i \sum_{i<j} \left[ \frac{p_{ij}^\alpha p_{ij}^\beta}{(1-p_{ij}^\alpha p_{ij}^\beta)^2} \right]}}. \quad (70)$$

–Under the ECM

Under the ECM, we can show that

$$\langle \min(w_{ij}^\alpha, w_{ij}^\beta) \rangle_{ECM} = \frac{p_{ij}^\alpha p_{ij}^\beta}{1 - r_{ij,\alpha} r_{ij,\beta}}, \quad (71)$$

where  $p_{ij}^\alpha = \frac{x_i^\alpha x_j^\alpha y_i^\alpha y_j^\alpha}{1 - y_i^\alpha y_j^\alpha + x_i^\alpha x_j^\alpha y_i^\alpha y_j^\alpha}$  as in Eq. (34), and  $r_{ij,\alpha} = y_i^\alpha y_j^\alpha$  as in Eq. (35).

The expectation of  $m_w^{\alpha,\beta}$  under the ECM is then given by

$$\langle m_w^{\alpha,\beta} \rangle_{ECM} = \frac{2 \sum_i \sum_{i<j} \frac{p_{ij}^\alpha p_{ij}^\beta}{1 - r_{ij,\alpha} r_{ij,\beta}}}{W^\alpha + W^\beta}. \quad (72)$$

The rescaled multiplexity under the ECM is therefore equal to

$$\mu_{ECM}^{\alpha,\beta} = \frac{2 \sum_i \sum_{i<j} \min\{w_{ij}^\alpha, w_{ij}^\beta\} - 2 \sum_i \sum_{i<j} \frac{p_{ij}^\alpha p_{ij}^\beta}{1 - r_{ij,\alpha} r_{ij,\beta}}}{W^\alpha + W^\beta - 2 \sum_i \sum_{i<j} \frac{p_{ij}^\alpha p_{ij}^\beta}{(1 - r_{ij,\alpha} r_{ij,\beta})}}. \quad (73)$$

In addition, we can show that

$$\sigma[\min\{w_{ij}^\alpha, w_{ij}^\beta\}]_{ECM} = \sqrt{\frac{p_{ij}^\alpha p_{ij}^\beta (1 - p_{ij}^\alpha p_{ij}^\beta + r_{ij,\alpha} r_{ij,\beta})}{(1 - r_{ij,\alpha} r_{ij,\beta})^2}}. \quad (74)$$

We obtain the z-score under the ECM as

$$z_{ECM}^{\alpha,\beta} = \frac{\sum_i \sum_{i<j} \min\{w_{ij}^\alpha, w_{ij}^\beta\} - \sum_i \sum_{i<j} \frac{p_{ij}^\alpha p_{ij}^\beta}{(1 - r_{ij,\alpha} r_{ij,\beta})}}{\sqrt{\sum_i \sum_{i<j} \left[ \frac{p_{ij}^\alpha p_{ij}^\beta (1 - p_{ij}^\alpha p_{ij}^\beta + r_{ij,\alpha} r_{ij,\beta})}{(1 - r_{ij,\alpha} r_{ij,\beta})^2} \right]}}. \quad (75)$$

### III. FINDINGS

In our study, bank-firm credit relationships are obtained from the so-called SABI database (Sistema de Análisis de Balances Ibéricos [6]) by Bureau van Dijk. The data set consists of 193 banks and 202,691 firms in 2007 (firms located in 60 industry sectors [7]). Our procedure for the analysis of multilayer bank-firm credit network is organized as follows. First, we will provide an overview of the original bipartite bank-firm credit network as well

the bank-sector credit network. In the next step, we break down firms into sectors based on the associated industrial sector codes, and then use the projection method to derive the matrices of overlaps between banks.

Note that we treat each of 60 industrial sectors as a separate layer. Considering a system of networks rather than the aggregate of all credit relations reflects the fact that firms in different sectors may have different characteristics like sector-specific risk, firm sizes, etc., and that banks may consider the sector that a borrower is located in as one of their criteria for screening. In each layer, we obtain two versions of projection networks, the binary version indicating whether two banks lend to at least one common firm, and the weighted version showing how many firms each pair of two banks co-finances. We then investigate the overlaps and dependencies between layers based on the measures for multiplexity introduced in the previous section, for both the binary as well as weighted cases.

#### A. Phenomenology to the bank-firm credit network of Spain

We report some basic statistics for the diversification of banks, firms, and sectors based on their degrees in Table (I). The distributions of banks' degree  $k_{bf}$ , firms' degree  $k_{fb}$ , and lending relations to sectors  $k_{bs}$  are shown in Figure 1. We observe that the distribution of banks' degree is much wider than that of firms' degree. While many banks diversify their lending serving often more than 1000 firms, almost all firms concentrate their borrowing on 1 to 3 banks (see panels (a), (b) of Figure 1). In addition, lending is heterogeneously distributed across sectors, as shown in the panel (c) of Figure 1.

	Degrees	min	max	avg.	std.
$k_{bf}$	1	47075	1771	5877	
$k_{fb}$	1	8	1.68	0.93	
$k_{bs}$	1	59	22.71	18.11	
$k_{sb}$	1	162	73.06	40.98	

TABLE I: Basic statistics for the diversification of banks, firms, and sectors in 2007.

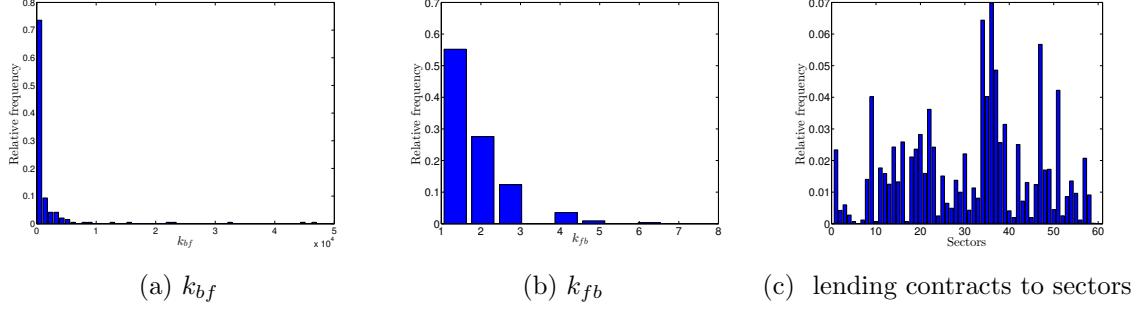


FIG. 1: Distributions of banks' degree, firms' degree, and lending relations to sectors in 2007. Panel (a) banks' degree  $k_{bf}$ . Panel (b) firms' degree  $k_{fb}$ . Panel (c) lendings to sectors.

In Figure 2 (a) we exhibit the relation between  $\log(k_{bf})$  and  $k_{bs}$ . It shows that a high number of firms that a bank lends to will also correspond to a high level of sector diversification of that bank [8]. In contrast, banks with smaller degrees concentrate their lending on a limited number of sectors.

For each sector, let  $k_{sf}$  denote the number of firms in that sector that borrow from all banks [9]. In Figure 2 (b), a positive correlation between  $\log(k_{sf})$  and  $\log(k_{sb})$  is found, suggesting that in terms of log-log scale, a large (small) number of firms borrowing from banks reveals a high (low) level of sectors' borrowing diversification.

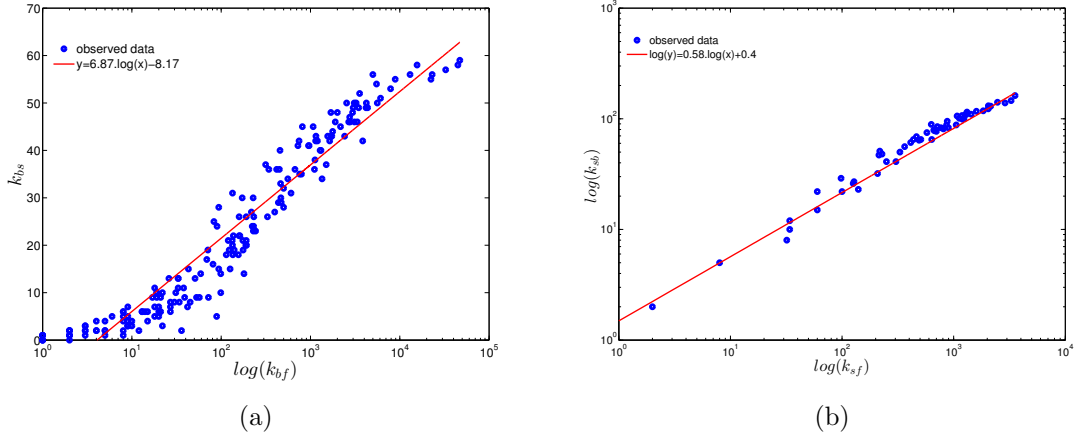


FIG. 2: Bank's diversification and sector's diversification in 2007. Panel (a) the lending to sectors ( $k_{bs}$ ) vs. the lending to firms ( $k_{bf}$ ) in semilogx plot. Panel (b) the number of banks lending to each sector ( $k_{sb}$ ) vs. the number of firms in that sector borrowing from banks ( $k_{sf}$ ) in log-log scale.

The results show the relevance of the presence of sector specific layers in the bank-firm

credit network of Spain. In the following subsections, we will focus on the overlaps and the correlations between layers in different versions (i.e. the binary and weighted versions) of the network.

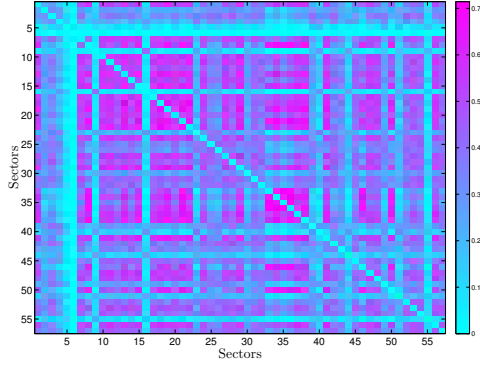
## B. Binary analysis

For the binary version, we show the raw binary multiplexity and its corresponding distribution respectively in Figure 3 (a) and Figure 3 (b). We find that, some of the layers exhibit a high correlation in their borrowing structure while other pairs show little overlap in their lender banks.

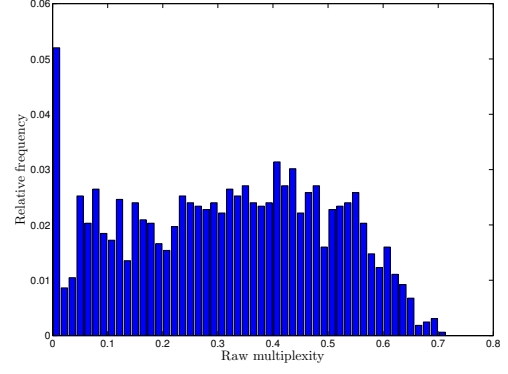
The rescaled multiplexity under the BRG model and its distribution are displayed in Figure 3 (c) and Figure 3 (d). In addition, at the bottom of Figure 3, in panels (e) and (f), we, respectively, display the rescaled multiplexity and the corresponding distribution under the BCM. Clearly, it is difficult to find significant differences between the rescaled quantities and the raw ones by mere inspection of these plots.

Next, since the analysis based on the color-coded multiplexity matrices does not allow any conclusion on the discrepancy of the observed values to the corresponding expected ones under the null models (e.g. Gemmetto and Garlaschelli, 2015; Gemmetto et al., 2015), we also exhibit z-scores evaluated under the BRG model and the BCM. More specifically, we plot z-scores against the rescaled multiplexity in the BRG model (Figure 4 (a)) and in the BCM (Figure 4 (b)). We observe that, in both null models, almost all z-scores are much higher than the critical value  $z^*=2$ . This indicates that, compared to both null models, our multilayer network in its binary version has a significant, non-random structure of correlations between layers.

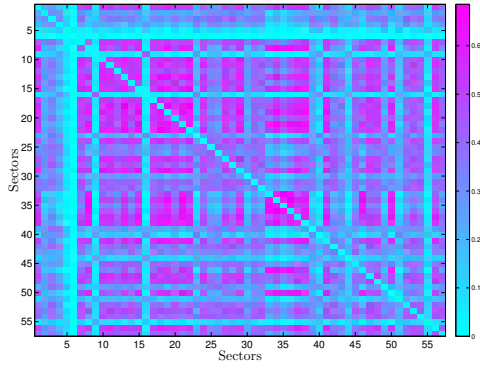
Moreover, a general positive correlation between  $z_{BRG}$  and  $\mu_{BRG}$  is clearly shown in Figure 4 (a), meaning that high (low)  $\mu_{BRG}$  corresponds to high (low)  $z_{BRG}$ . In Figure 4 (b), we also observe a similar correlation between z-scores and rescaled multiplexities under the BCM model. Furthermore, a majority of  $z_{BCM}$  are located in the interval  $[0, 40]$ , while almost all of the  $z_{RGM}$  are much larger than 40. This shows that for small values of multiplexity, the observed multiplexity deviates somewhat less on average from the expected multiplexity in the BCM than in the BRG model.



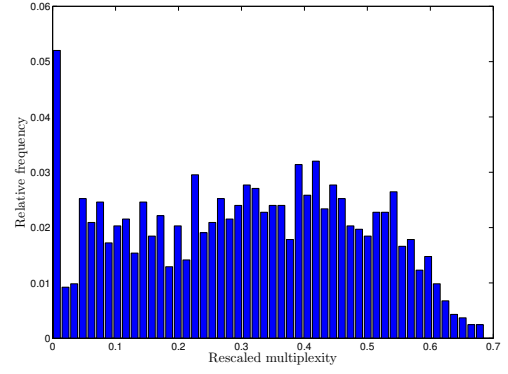
(a)  $m_{bin}$



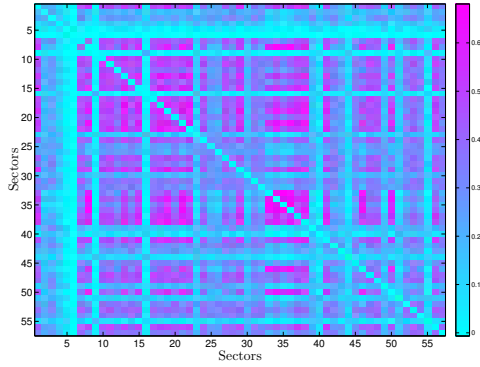
(b) Distribution of  $m_{bin}$



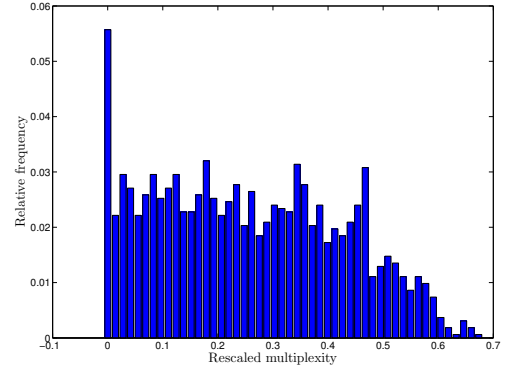
(c)  $\mu_{BRG}$



(d) Distribution of  $\mu_{BRG}$



(e)  $\mu_{BCM}$



(f) Distribution of  $\mu_{BCM}$

FIG. 3: Binary multiplexities between layers of the bank-firm credit network in 2007. Panels (a), (b): Raw multiplicity  $m_{bin}$  and the corresponding distribution. Panels (c), (d): Rescaled multiplicity under the BRG ( $\mu_{BRG}$ ) and the corresponding distribution. Panels (e), (f): Rescaled multiplicity under the BCM ( $\mu_{BCM}$ ) and the corresponding distribution.



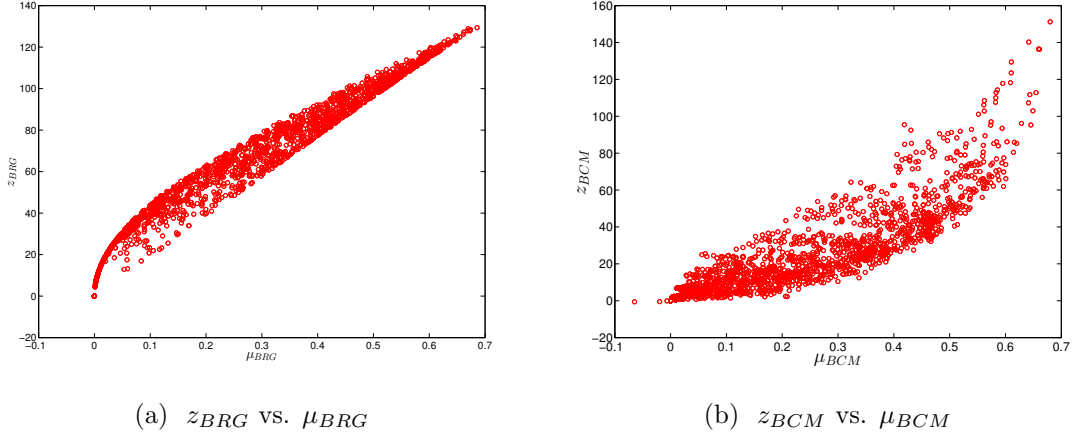


FIG. 4: Binary z-scores in 2007. Panel (a)  $z_{BRG}$  vs.  $\mu_{BRG}$ . Panel (b)  $z_{BCM}$  vs.  $\mu_{BCM}$ .

### C. Weighted analysis

We now move on to the analysis of the weighted version of the multilayer bank-firm credit network. To begin, in Figure 5, we compare the raw weighted multiplexity matrix with the raw binary multiplexity matrix, element by element. We find a tendency that levels of correlations between sectors in the weighted version are often smaller than in the binary version, indicating the role of the link intensity in weighted multiplexities.

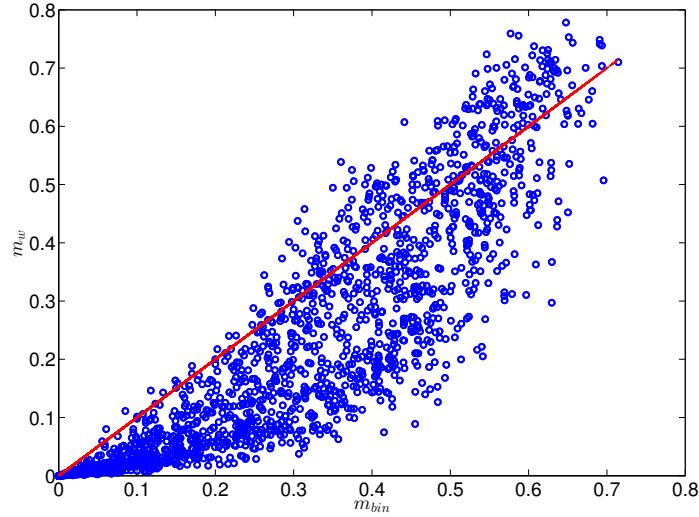


FIG. 5: Comparison between binary and weighted multiplexities, i.e.  $m_w$  vs.  $m_{bin}$ . The red line stands for the identity line. For almost all pairs of sectors we find that  $m_w < m_{bin}$ .

Next, we show the color-coded matrix of the raw weighted multiplexity and the corresponding distribution in the panels (a) and (b) of Figure 6. Similar to the binary version, we can see that the color-coded matrix as well as the distribution of the raw weighted multiplexity reveal a very hierarchical structure of correlations between layers. More specifically, on the one hand, a number of clusters of layers are highly correlated to each other, while on the other hand, many other pairs are characterized by very small (non-negative) values of multiplexity.

The rescaled multiplexities for the weighted version, i.e.  $\mu_{WRG}$  (under the WRG model),  $\mu_{WCM}$  (under the WCM), and  $\mu_{ECM}$  (under the ECM) and their corresponding distributions are shown from panels (c) to (h) of Figure 6. Regarding the WRG model, we find that there is no significant difference between  $m_w$  and  $\mu_{WRG}$  (see the panels (c) and (d) of Figure 6), pointing out that specifying only the information about the total weight in each layer is not enough to replicate the observed correlations between layers. This result is similar to what we have obtained from the comparison between the raw multiplexity and the rescaled one under the BRG model in the binary version.

In contrast, when the strength sequence is maintained in the WCM, in comparison between Figure 6 (a) and Figure 6 (e) as well as between Figure 6 (b) and Figure 6 (f), we find that the correlations between many sectors are partially reduced in  $\mu_{WCM}$ . In addition, compared to the WCM, although in the ECM the knowledge of the observed degree sequence in addition to the observed strength sequence in each layer of the observed multiplex network yields a slight improvement in replicating the elements of the weighted multiplexity matrix, significant correlations between some layers still emerge after filtering the effects of the local constraints (see Figure 6 (g) and Figure 6 (h)).

In Figure 7 (a), (b), and (c) we report the z-scores evaluated under the three null models in the weighted version. Similar to the relation between  $z_{BRG}$  and  $\mu_{BRG}$  in the BRG model, we also observe an overall positive correlation between  $z_{WRG}$  and  $\mu_{WRG}$ . This implies that high values of  $\mu_{WRG}$  correspond to large discrepancies between the observed multiplexity  $m_w$  and the expected one obtained from the WRG model, and vice-versa. In contrast, under the WCM and the ECM, it becomes more difficult to detect any overall significant correlation between the elements of the rescaled multiplexity matrix and the corresponding z-scores, since now both low as well as high levels of rescaled multiplexities can have high z-scores. However, it is worthwhile to emphasize that for  $\mu_{WCM} > 0.2$  or  $\mu_{ECM} > 0.2$ , the values of

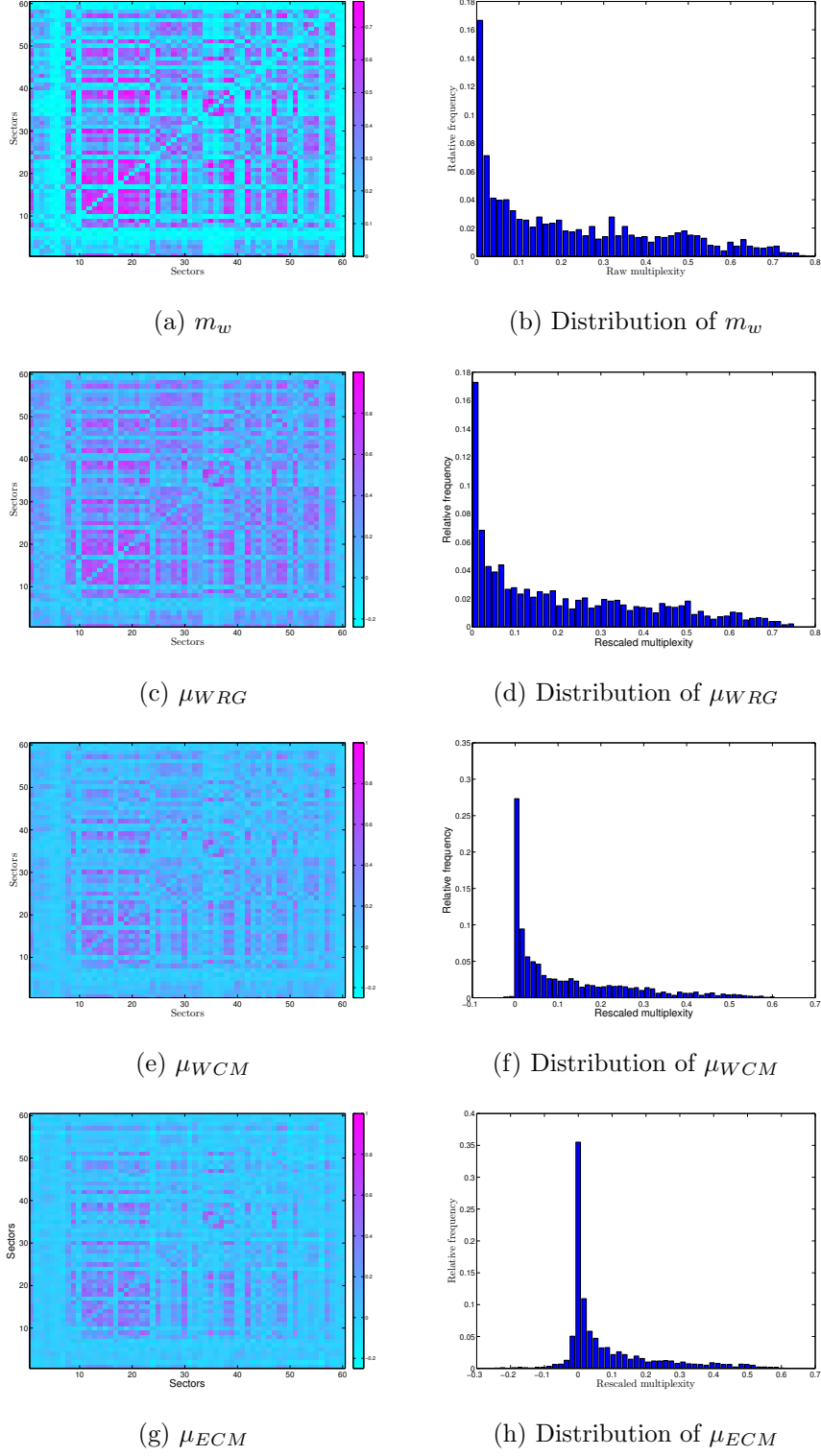


FIG. 6: Weighted multiplicities between layers of the bank-firm credit network of Spain in 2007. Panels (a), (b):  $m_w$  and the corresponding distribution. Panels (c), (b):  $\mu_{WRG}$  and the corresponding distribution. Panels (e), (f):  $\mu_{WCM}$  and the corresponding distribution. Panels (g), (h):  $\mu_{ECM}$  and the corresponding distribution.

the corresponding z-scores are also typically higher than the critical value  $z^*=2$ .

In addition, among the three null models, the absolute value of z-scores under the WRG is usually much larger than the corresponding ones evaluated under the WCM and the ECM. In particular, we find that, on the one hand,  $-1 < z_{WCM} < 10$  and  $-6 < z_{ECM} < 12$ ; on the other hand, almost all of  $z_{WRG}$  are greater than 50. That means, overall, the observed multiplexity deviates less from the expected multiplexity under the WCM and under the ECM than under the WRG model.

We should emphasize that, in all three null models employed for the weighted version, many z-scores (especially for the ones associated with high values of the rescaled multiplexity) are larger than the critical value  $z^*=2$ , showing that the weighted version of the network does display a significant, non-random structure of correlations between layers.

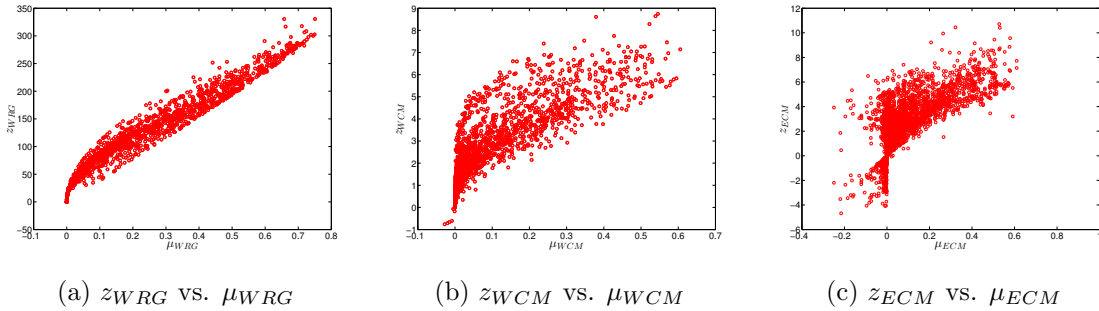


FIG. 7: Weighted z-scores in 2007. Panel (a)  $z_{WRG}$  vs.  $\mu_{WRG}$ , panel (b)  $z_{WCM}$  vs.  $\mu_{WCM}$ , panel (c)  $z_{ECM}$  vs.  $\mu_{ECM}$ .

#### D. Hubs distribution and hidden variables

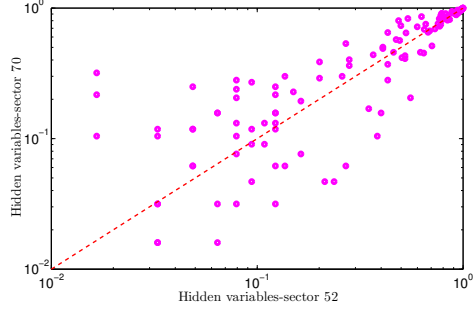
Recalling Eq. (26), given two nodes in any layer associated with two hidden variables  $(x, y)$  extracted under the BCM, the probability of a link between them is equal to  $\frac{xy}{xy+1}$ . Similarly, from Eq. (30), given two nodes in any layer associated with two hidden variables  $(z, t)$  extracted from the WCM, the expected weight between them is  $\frac{zt}{1-zt}$ . It is easy to show that  $\frac{xy}{xy+1}$  is an increasing function of  $x$  and  $y$  in  $(0, \infty)$ , and  $\frac{zt}{1-zt}$  is also an increasing function of  $z$  and  $t$  in  $[0, 1)$ . Therefore, in each layer, nodes associated with a higher level of hidden variables will attract more links (in the BCM) or more weights (in the WCM) from other nodes. When looking across layers, obviously if the order of hidden variables in a layer  $\alpha$  (i.e.  $\{x_i^\alpha\}_{i=1}^N$ ) is similar to the order of hidden variables in another layer  $\beta$  (i.e.  $\{x_i^\beta\}_{i=1}^N$ ),

this will lead to a higher overlap and correlation between these two layers.

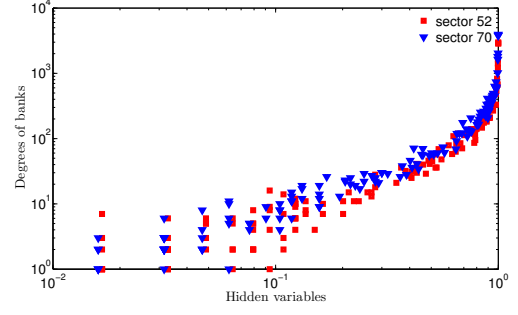
In the bank-firm credit network of Spain, similar to what is observed in the case of the International Trade Network (see Gemmetto and Garlaschelli, 2015), we find that a number of pairs of sectors share the same hubs. This may partially explain why these sectors exhibit more overlap and correlation. In Figure 8 we show an example of the distribution of hubs in the pair of layers that have the highest value of the weighted multiplexity, i.e. the layer associated with the industrial sector coded 52 (namely layer 52) and the layer associated with the industrial sector coded 70 (namely layer 70). According to the classification based on NACE (Rev. 2), the former corresponds to the industry of warehousing and support activities for transportation, and the latter corresponds to the industry of activities of head offices and management consultancy activities.

Let  $\{x_i^{52}\}_{i=1}^N$  and  $\{x_i^{70}\}_{i=1}^N$  be hidden variables obtained from the WCM model in these two layers. As shown in Figure 8 (a), we observe that banks with higher values of  $x_i^{52}$  also tend to have higher values of  $x_i^{70}$ . We then investigate the relation between hidden variables and the degree of banks in the original bipartite structure, i.e. total number of borrowers of banks in each sector. Figure 8 (b) shows that in each layer, a larger value of hidden variables reveals a higher degree of banks, and vice-versa. Figure (9) visualizes the bank-bank projection networks in the layer 52 and the layer 70. Size and color of each node are proportional to its degree in each layer. A close inspection of the center of each panel shows that both layers share a certain number of common hubs. It should be emphasized that we also typically observe this behavior in other pairs of highly correlated layers.

Obviously, since many significant correlations are still present after filtering the effects of the various constraints in all layers, other factors than the distribution of hubs across layers should be studied further. Such factors may be associated with higher-order topological properties of the network and/or non-topological properties of banks, sectors, and firms.

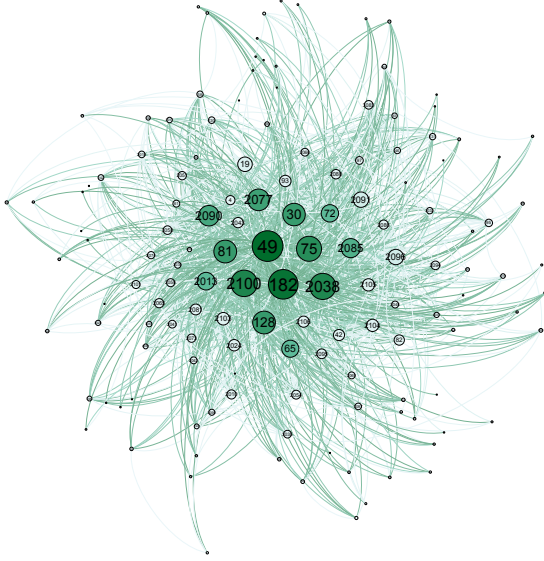


(a) Hidden variables in layers 52 and 70

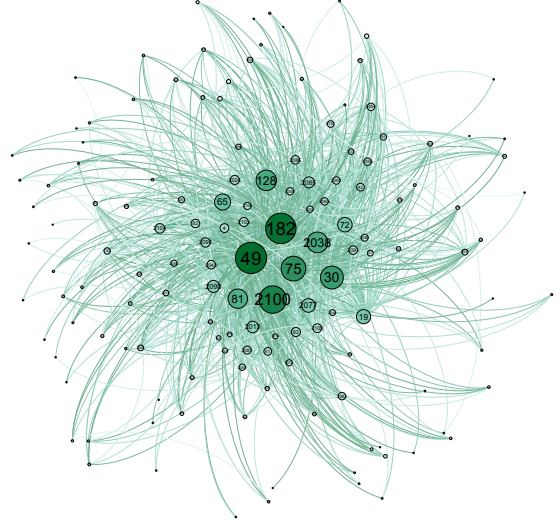


(b) Hidden variables and bank degrees

FIG. 8: Hubs and hidden variables in the two example layers 52 and 70. Panel (a):  $x_i^{70}$  vs.  $x_i^{52}$ , where the red-dashed line stands for the identity line. Panel (b): bank degrees vs. hidden variables in the two layers 52 and 70.



(a) Layer 52



(b) Layer 70

FIG. 9: Common hubs in the two example layers 52 (panel a) and 70 (panel b). Nodes represent banks. Size and color of a node are proportional to its degree in that layer; the number associated with each node is the bank code in the data set.

#### IV. CONCLUSIONS

We have applied recent advances in measuring overlaps and correlations between layers in multilayer networks to the bank-firm credit network of Spain, for both the binary as well as weighted versions. Each layer represents an industrial sector where firms (i.e. borrowers) are located in. We find that, first, the dependencies between layers of the observed network are highly heterogeneous. In such a hierarchical structure, layers in some clusters are highly overlapped and correlated to each other, whereas many other pairs of layers exhibit only a small level of overlaps and correlations.

Second, comparing the observed multiplexities to the expected ones obtained from the various null models maintaining different fundamental constraints in each layer, we find that there is no significant difference between the observed multiplexities and the rescaled ones filtering out the effects of the global constraints, indicating that these constraints play no significant role in the cross-layer dependencies of the observed network. When the role of local constraints is taken into account, on the one hand, in the binary version, almost all correlations are still present after subtracting the effects of the observed degree sequences in all layers. On the other hand, when filtering the effects of the heterogeneity in the observed strength and/or degree sequences in all layers, the weighted multiplexities are partially reduced. However, many significant correlations still emerge after filtering, implying that the observed network does display a non-random structure of dependencies between layers that can not simply be explained by more primitive properties of the network alone. In particular, in both versions of the network, a significant deviation from all null models is always observed in the highest level of dependencies between layers. Furthermore, interestingly, in the weighted version, many smaller values of multiplexities also strongly deviate from the expected ones evaluated under the various weighted null models.

Our study contributes to the existing literature on the role of the different fundamental constraints in the overlaps and correlations between layers of multilayer networks. Since the method used in this study is generic, we suggest that future studies should also consider to investigate the structural overlaps and dependencies in other multilayer financial networks, for instance in networks where different types of assets or financial transactions represent different layers.

Moreover, in our study, each layer is analyzed in forms of the one-mode projection network

of the banking sector that it generates. Similarly, in the previous studies of Barigozzi et al. (2015), Gemmetto and Garlaschelli (2015), and Gemmetto et al. (2015), each layer is also studied in forms of the one-mode networks. In contrast, up till now, the role of constraints in the original bipartite structure of single layers has received little attention. Since the one-mode projection network is always less informative than the original bipartite network (e.g. Lehmann et al., 2008; Luu and Lux, 2016) we believe that further research considering the bipartite structure in each layer may provide a more comprehensive analysis of the role of the different fundamental constraints in the multilayer structure of real bank-firm credit networks. In that research direction, the null models defined for bipartite networks should be employed (e.g. see Saracco et al., 2015; Di Gangi et al., 2015; Luu and Lux, 2016).

## V. REFERENCES

- Aldasoro I., Alves I. 2015. Multiplex interbank networks and systemic importance: An application to European data. SAFE Working Paper No. 102. Available at: <http://ssrn.com/abstract=2603732>.
- Bargigli L., di Iasio G., Infante L., Lillo F., Pierobon F. 2015. The multiplex structure of interbank networks. *Quantitative Finance* 15 (4), pp. 673-691.
- Barigozzi M., Fagiolo G., Garlaschelli D. 2010. Multinetwork of international trade: A commodity-specific analysis. *Physical Review E* 81 (4).
- Bianconi G. 2013. Statistical mechanics of multiplex ensembles: Entropy and overlap. *Physical Review E* 87 (6).
- Bianconi G. 2014. Multilayer networks: Dangerous liaisons?. *Nature Physics* 10, pp. 712-714.
- Boccaletti S., Bianconi G., Criado R., del Genio C. I., Gomez-Gardenes J., Romance M., Sendina-Nadal I., Wang Z., Zanin M. 2014. Structure and dynamics of multilayer networks. *Physics Reports* 544 (1), pp. 1-122.
- Caccioli F., Shrestha M., Moore C., Farmer J. D. 2014. Stability analysis of financial contagion due to overlapping portfolios. *Journal of Banking and Finance* 46, pp. 233-245.
- Chen Y. -Z., Huang Z. -G., Zhang H. -F., Eisenberg D., Seager T. P., Lai Y. -C. 2015. Extreme events in multilayer, interdependent complex networks and control. *Scientific Reports* 5.



- De Masi G., Gallegati M. 2012. Bank-firms topology in Italy. *Empirical Economics* 43 (2), pp. 851-866.
- De Masi G., Fujiwara Y., Gallegati M., Greenwald B., Stiglitz J. E. 2011. An analysis of the Japanese credit network. *Evolutionary and Institutional Economics Review* 7 (2), pp. 209-232.
- Di Gangi D., Lillo F., Pirino D. 2015. Assessing systemic risk due to fire sales spillover through maximum entropy network reconstruction. Working Paper. Available at: [arXiv:1509.00607](https://arxiv.org/abs/1509.00607).
- Gemmetto V., Garlaschelli D. 2015. Multiplexity versus correlation: the role of local constraints in real multiplexes. *Scientific Reports* 5.
- Gemmetto V., Squartini T., Picciolo F., Ruzzenenti F., Garlaschelli D. 2015. Multiplexity and multireciprocity in directed multiplexes. Working Paper. Available at: [arXiv:1411.1282](https://arxiv.org/abs/1411.1282).
- Huang X., Vodenska I., Havlin S., Stanley H. E. 2013. Cascading failures in bi-partite graphs: Model for systemic risk propagation. *Scientific Reports* 3.
- Illueca M., Norden L., Udell G. F. 2013. Liberalization and risk-taking: Evidence from government-controlled banks. *Review of Finance* 18 (4), pp. 1217-1257.
- Kivela M., Arenas A., Barthelemy M., Gleeson J. P., Moreno Y., Porter J. P. 2014. Multilayer networks. *J. Complex Networks* 2 (3), pp. 203-271.
- Lehmann S., Schwartz M., Hansen L. K. 2008. Biclique communities. *Physical Review E* 78 (1).
- Luu D. T., Lux T. 2016. Identifying patterns in the bank-sector credit network of Spain. Working Paper.
- Lux T. 2016. A model of the topology of the bank-firm credit network and its role as channel of contagion. *Journal of Economic Dynamics and Control* 66, pp. 36-53.
- Mastrandrea R., Squartini T., Fagiolo G., Garlaschelli D. 2014a. Enhanced reconstruction of weighted networks from strengths and degrees. *New Journal of Physics* 16.
- Mastrandrea R., Squartini T., Fagiolo G., Garlaschelli D. 2014b. Reconstructing the world trade multiplex: The role of intensive and extensive biases. *Physical Review E* 90 (6).
- Menichetti G., Remondini D., Panzarasa P., Mondragón R. J., Bianconi G. 2014. Weighted multiplex networks. *PLoS ONE* 9 (6).
- Menichetti G., Remondini D., Bianconi G. 2014. Correlation between weights and overlap

in ensembles of weighted multiplex networks. *Phys. Rev. E* 90 (6).

Menichetti G., Dall'Asta L., Bianconi G. 2016. Control of multilayer networks. *Scientific Reports* 6.

Poledna S., Molina-Borboa J. L., Martínez-Jaramillo S., van der Leij M., Thurner S. 2015. The multi-layer network nature of systemic risk and its implications for the costs of financial crises. *Journal of Financial Stability* 20, pp. 70-81.

Saracco F., Clemente R. D., Gabrielli A., Squartini T. 2015. Randomizing bipartite networks: the case of the World Trade Web. *Scientific Reports* 5.

Squartini T., Fagiolo G., Garlaschelli D. 2011a. Randomizing world trade: I. A binary network analysis. *Phys. Rev. E* 84 (4).

Squartini T., Fagiolo G., Garlaschelli D. 2011b. Randomizing world trade: II. A weighted network analysis. *Phys. Rev. E* 84 (4).

Squartini T., Garlaschelli D. 2011. Analytical maximum-likelihood method to detect patterns in real networks. *New Journal of Physics* 13.

Squartini T., Mastrandrea R., Garlaschelli D. 2015. Unbiased sampling of network ensembles. *New Journal of Physics* 17.

## VI. APPENDIX

In this section we will show that under the ECM, for every pair of two layers  $\alpha, \beta$ , the expectations  $\langle \min(w_{ij}^\alpha, w_{ij}^\beta) \rangle_{ECM}$ ,  $\langle \min(w_{ij}^\alpha, w_{ij}^\beta)^2 \rangle_{ECM}$ , and consequently the standard deviation  $\sigma[\min(w_{ij}^\alpha, w_{ij}^\beta)]_{ECM}$  can analytically be calculated via hidden variables extracted from the observed degree as well as strength sequences in the two layers. That will lead to the expressions for  $\langle m_w^{\alpha, \beta} \rangle_{ECM}$ ,  $\mu_{ECM}^{\alpha, \beta}$ , and  $z_{ECM}^{\alpha, \beta}$  as respectively shown in Eqs. (72), (73), and (75) in the main text. For the proofs under other null models including the BRG model, the BCM, the WRG model, and the WCM, we refer the readers to the study of Gemmetto and Garlaschelli (2015).

First, we will start with some relevant lemmas used in our proof.

For  $0 < y < 1$  we have:

### Lemma 1

$$\sum_{n=0}^{\infty} y^n = \frac{1}{(1-y)}. \quad (76)$$

Eq. (76) leads to

**Lemma 2**

$$\sum_{n=0}^{\infty} n y^n = \frac{y}{(1-y)^2}. \quad (77)$$

From Eq. (77) we have

**Lemma 3**

$$\sum_{n=0}^{\infty} n^2 y^n = \frac{y^2 + y}{(1-y)^3}. \quad (78)$$

From Eqs. (76), (77), and (78) we have:

**Lemma 4**

$$\sum_{n=0}^{\infty} n(y^{n-1} - y^n) = \frac{1}{(1-y)}, \quad (79)$$

and

**Lemma 5**

$$\sum_{n=0}^{\infty} n^2 y^{n-1} - n^2 y^n = \frac{y+1}{(1-y)^2}. \quad (80)$$

As shown in the main text, in the ECM, with hidden variables  $\{x_i^\alpha\}_{i=1}^N$  and  $\{y_i^\alpha\}_{i=1}^N$  extracted from the observed degree and strength sequences in each layer  $\alpha$  (see Sys. (32)), the probability of a link between node  $i$  and node  $j$  is

$$p_{ij}^\alpha = \frac{x_i^\alpha x_j^\alpha y_i^\alpha y_j^\alpha}{1 - y_i^\alpha y_j^\alpha + x_i^\alpha x_j^\alpha y_i^\alpha y_j^\alpha} \quad (81)$$

and probability of a link of weight  $w_{ij}^\alpha$  between node  $i$  and node  $j$  is

$$q(w_{ij}^\alpha) = \begin{cases} 1 - p_{ij}^\alpha, & \text{if } w_{ij}^\alpha = 0 \\ p_{ij}^\alpha r_{ij,\alpha}^{w_{ij}^\alpha - 1} (1 - r_{ij,\alpha}), & \text{if } w_{ij}^\alpha > 0 \end{cases} \quad (82)$$

where  $r_{ij,\alpha} = y_i^\alpha y_j^\alpha$ .

Considering that weights are integers, we obtain the CCDF of a link of weight  $w_{ij}^\alpha$  as

$$q(w_{ij}^\alpha \geq w) = 1 - \sum_0^{w-1} q_{ij}(t). \quad (83)$$

It follows from Eq. (82) and Eq. (83) that the CCDF of a link of weight  $w_{ij}^\alpha$  can be rewritten as

$$q(w_{ij}^\alpha \geq w) = 1 - [1 - p_{ij}^\alpha + \sum_{t=1}^{w-1} p_{ij}^\alpha (r_{ij,\alpha}^{t-1} - r_{ij,\alpha}^t)] = p_{ij}^\alpha r_{ij,\alpha}^{w-1}. \quad (84)$$

From (84), we have

$$q(\min(w_{ij}^\alpha, w_{ij}^\beta) \geq w) = q(w_{ij}^\alpha \geq w)q(w_{ij}^\beta \geq w) = (p_{ij}^\alpha r_{ij,\alpha}^{w-1})(p_{ij}^\beta r_{ij,\beta}^{w-1}). \quad (85)$$

Note that, the expected value of  $\min(w_{ij}^\alpha, w_{ij}^\beta)$  under ECM model can be formulated as

$$\langle \min(w_{ij}^\alpha, w_{ij}^\beta) \rangle_{ECM} = \sum_{w'} w' q(\min(w_{ij}^\alpha, w_{ij}^\beta) \geq w') - w' q(\min(w_{ij}^\alpha, w_{ij}^\beta) \geq (w' + 1)). \quad (86)$$

From Lemma 4 (Eq. (79)), Eq. (85) and Eq. (86), we get

$$\langle \min(w_{ij}^\alpha, w_{ij}^\beta) \rangle_{ECM} = p_{ij}^\alpha p_{ij}^\beta \sum_{w'=0}^{\infty} w' [(r_{ij,\alpha} r_{ij,\beta})^{w'-1} - (r_{ij,\alpha} r_{ij,\beta})^{w'}] = \frac{p_{ij}^\alpha p_{ij}^\beta}{1 - r_{ij,\alpha} r_{ij,\beta}}. \quad (87)$$

( $\Rightarrow$  **Eq. (71) in the main text is proved!**)

Note that, with a similar approach we have

$$\langle \min(w_{ij}^\alpha, w_{ij}^\beta)^2 \rangle_{ECM} = \sum_{w'=0}^{\infty} w'^2 [q(\min(w_{ij}^\alpha, w_{ij}^\beta) \geq w') - q(\min(w_{ij}^\alpha, w_{ij}^\beta) \geq w' + 1)]. \quad (88)$$

or equivalently

$$\langle \min(w_{ij}^\alpha, w_{ij}^\beta)^2 \rangle_{ECM} = p_{ij}^\alpha p_{ij}^\beta \sum_{w'=0}^{\infty} w'^2 [(r_{ij,\alpha} r_{ij,\beta})^{w'-1} - (r_{ij,\alpha} r_{ij,\beta})^{w'}]. \quad (89)$$

From Lemma 5 (Eq. (80)) and Eq. (89), we obtain

$$\langle \min(w_{ij}^\alpha, w_{ij}^\beta)^2 \rangle_{ECM} = \frac{p_{ij}^\alpha p_{ij}^\beta (r_{ij,\alpha}^\alpha r_{ij,\beta}^\beta + 1)}{(1 - r_{ij,\alpha} r_{ij,\beta})^2}. \quad (90)$$

In addition, from Eq. (87) we have

$$\langle \min(w_{ij}^\alpha, w_{ij}^\beta) \rangle^2 = \left( \frac{p_{ij}^\alpha p_{ij}^\beta}{1 - r_{ij,\alpha} r_{ij,\beta}} \right)^2. \quad (91)$$

Therefore, from Eqs. (89), (91), the variance of  $\min(w_{ij}^\alpha, w_{ij}^\beta)$  is specified as

$$\sigma(\min(w_{ij}^\alpha, w_{ij}^\beta))_{ECM}^2 = \frac{p_{ij}^\alpha p_{ij}^\beta (r_{ij}^\alpha r_{ij}^\beta + 1)}{(1 - r_{ij,\alpha} r_{ij,\beta})^2} - \left( \frac{p_{ij}^\alpha p_{ij}^\beta}{1 - r_{ij,\alpha} r_{ij,\beta}} \right)^2 = \frac{p_{ij}^\alpha p_{ij}^\beta (1 - p_{ij}^\alpha p_{ij}^\beta + r_{ij,\alpha} r_{ij,\beta})}{(1 - r_{ij,\alpha} r_{ij,\beta})^2}. \quad (92)$$

( $\Rightarrow$  **Eq. (74) in the main text is proved!**)

- 
- [1] In fact, there are also several attempts on analyzing multilayer financial networks, such as Aldasoro and Alves (2015), Bargigli et al. (2015), and Poledna et al. (2015). They also suggest that the multilayer nature of financial networks should be taken into account instead of analyzing aggregate or single-layer networks. In their studies, the classification of layers is often based on direct relations/transactions between banks. In contrast, we focus on the multilayer structure of joint exposures of banks when lending to non-financial firms in different industrial sectors.
  - [2] For more detailed analyses of the evolution of the bank-firm credit market and the bank-sector credit network of Spain, we refer the readers to, for example, Illueca et al. (2013) and Luu and Lux (2016).
  - [3] We refer the readers to the papers of Bianconi (2013) and Menichetti et al. (2014) for a more detailed description of the multiplexity and overlaps in a multilayer network. A more comprehensive review on multilayer networks can be found in the study of Kivela et al. (2014), for instance.
  - [4] Throughout this paper,  $\langle X \rangle_Y$  is the notation for expectation of  $X$  under the referenced null model  $Y$ .
  - [5] Throughout this paper,  $z[X]_Y$  and  $\sigma[X]_Y$  are respectively the notations for standard deviation and  $z$  score of  $X$  under the referenced null model  $Y$ .
  - [6] See, for instance, the introduction to SABI by Bureau van Dijk at:  
<http://www.bvdinfo.com/en-gb/our-products/company-information/national-products/sabi>.
  - [7] Sector codes are based on “The Statistical Classification of Economic Activities in the European Community” (NACE), level 2, which is identified by two-digit numerical codes (01 to 99).
  - [8] Note that the estimated parameters in this Figure are just used for the purpose of illustration of the correlations between  $k_{bs}$  and  $k_{bf}$  in panel (a) as well as between  $k_{sb}$  and  $k_{sf}$  in panel (b).

[9] Here we assume that  $k_{sf}$ , i.e. the number of firms in each sector financed by all banks, is a proxy for sectors' borrowing demand.